Alloying in Ge(Si)/Si(001) self-assembled islands during their growth and capping: XPS and AFM study

M. De Seta, G. Capellini,* and F. Evangelisti
Dipartimento di Fisica "E. Amaldi," Università Roma Tre, Via della Vasca Navale 84, 00146 Roma, Italy
(Received 7 August 2007; revised manuscript received 21 December 2007; published 29 January 2008)

In this paper, we present a study on the Ge composition and shape evolution of self-assembled Ge/Si(001) islands during the island growth and the subsequent Si capping at 750 °C. By combining atomic force microscope images and x-ray photoemission spectroscopy data, we quantitatively determine the Ge distribution in the wetting layer and in the islands, *separately*. We found that in as-grown sample, the wetting layer is substantially Si-richer than the islands, its average composition being independent of the growth rate. Upon capping, the islands proceed to a reverse Stranski-Krastanov shape evolution, with a progressive Si enrichment of both the wetting layer and the islands. We demonstrate that this evolution occurs at *constant* island volume. The observed behavior indicates the suppression of the lateral diffusion of both Ge and Si atoms from the wetting layer to the surface of the enlarging islands, and vice versa.

DOI: 10.1103/PhysRevB.77.045431 PACS number(s): 68.65.Hb, 81.70.Jb, 81.07.Ta, 68.37.Ps

I. INTRODUCTION

Strained Ge/Si(001) self-assembled islands have been investigated extensively by many research groups in recent years due to their potential applications in optoelectronic devices.[1,2] The optoelectronic properties of such systems are strongly related to the island composition and shape. These features are, in turn, influenced by the intermixing of Si and Ge atoms occurring both during the Ge island growth[3,4] and the island capping with a silicon layer.[5–8] As a matter of fact, intermixing is a competitive mechanism reducing the strain in heteroepitaxy and must, therefore, be included in each comprehensive model describing island growth or postgrowth processes, such as island annealing or capping.[9–12] Recently, theoretical studies have indicated intermixing between surface and subsurface layers to be the key factor controlling the transition from planar growth to island formation.[13] Intermixing was shown to influence drastically the shape and size of self-assembled islands during the growth and postgrowth annealing. The relative prevalence of thermodynamic and kinetic effects is still under debate, and the effects of deposition temperature, growth rate, and the presence of carrier gases on the alloying have been the subject of a wealth of studies.[14] Although it has also been established that the island shape and composition change dramatically as a function of Si flux in a large range of deposition temperatures and growth rates, the evolution of Ge(Si) island shape and composition under Si capping is still under debate. Atomic force microscopy (AFM) and/or scanning tunneling microscopy images indicated that this interdiffusion was accomplished by island flattening and enlargement, in quantitative agreement with the strain relaxation due to the lower Ge content measured in the island during the capping process. In these works, constant or slightly increasing island volume combined with increasing coverage of the silicon cap layer has been measured by AFM.

On the other hand, in a recent work, Lang *et al.*[15] observed in real time, by means of *in situ* cross-section transmission electron microscopy, shrinkage of the Ge island during Si capping at a temperature in the 550–600 °C range. They attributed this phenomenon to the diffusion of Ge atoms from islands into the wetting layer (WL). Although they did not provide evidence of a WL dilution during the capping, they suggested that the Ge flux is promoted by the dropping of the Ge concentration in the WL below the critical value for island formation.[13] Katsaros *et al.*,[16] by combining wet etching and AFM measurements, have shown that after being capped at 580 °C, the volume of the Ge buried islands with a Ge content higher than 20% is reduced by more than half, while the island shape remains unchanged at 350 and 450 °C. Comparing island shape and morphology of the surface during the capping process, they also conclude that depending on the growth conditions, the surface morphology of the capped island layer can be radically different from the morphology of the buried islands. Similar conclusions were previously reported by two groups:[7,17] the presence of three-dimensional (3D) structures on the capping layer surface during the growth of the silicon capping layer at high rate and low temperature was attributed to the kinetically limited conformal growth of a silicon layer above the islands.

It is clear that the main problem to overcome in order to understand the island evolution during the capping process is the simultaneous monitoring of the actual island shape and of the Ge content, both in the islands and in the WL. In this work, we characterize the samples both by AFM and x-ray photoemission spectroscopy (XPS). In particular, the Ge($2p$) photocurrent signal that depends on the Ge atomic distribution within the first 0–1 nm below the free surface is measured, which allows us to check whether the surface morphology measured by AFM is that of "bare" intermixed islands or if it corresponds to the development of Si layers on top of the intermixed islands. By combining AFM and XPS measurements [involving the more bulklike Ge($3d$) photocurrent signal],[3,6,18] we quantify SiGe intermixing in the epilayer, taking into account that the average composition of the WL and the islands can be different. For this purpose, we deposited two Ge/Si(001) island samples at different growth rates so as to vary the surface coverage of the islands and, consequently, the contribution of the island-to-WL ratio to

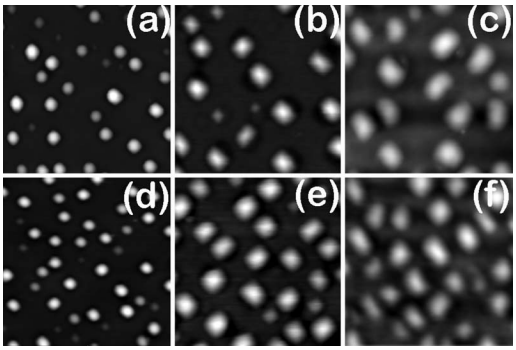

FIG. 1. $1.5\times1.5\ \mu m^2$ AFM images of samples belonging to series A (top line) and B (bottom line): [(a) and (d)] $\theta_{Si}=0$, (b) $\theta_{Si}=1.5$ nm, (e) $\theta_{Si}=1.8$ nm, and [(c) and (f)] $\theta_{Si}=4.5$ nm. Image sides are aligned along the [011]-equivalent directions.

the average island layer composition. We then investigated the shape and compositional evolution of these samples during silicon capping at 750 °C.

II. EXPERIMENT

The samples were deposited in an ultrahigh vacuum chemical vapor deposition cold-wall chamber using high purity silane and germane. The system base pressure was in the 1×10^{-10} Torr range and no carrier gas was used. The Si(001) substrates were degreased using a standard wet etch and then *in situ* cleaned by a 5 min exposure to H_2 atmosphere at 1100 °C. Subsequently, a 500-nm-thick Si buffer layer was deposited at a temperature $T_{dep}=800$ °C in order to recover a flat (2×1)-reconstructed silicon surface. Two sample series were prepared covering a Ge layer with a silicon cap layer of variable thickness θ_{Si} (0–18 nm). Both the islands and the capping layer were deposited at $T_{dep}=750$ °C. The Ge island layers, nominally identical in all the samples belonging to a given series, were deposited using two different growth rates: A series, $F^A=0.6$ Å/s; B series, $F^B=1.2$ Å/s. The Ge deposition time in the two series was tuned in order to have similar island shape and volume distributions in the uncapped samples.

The sample morphology was investigated by means of a Veeco CP-II AFM, operating in contact mode using high aspect ratio tips with a nominal tip radius of 5 nm. Finite tip-size convolution effects were taken into account in the analysis.

In situ XPS measurements were performed using a monochromatic Al $K\alpha$ source. The photocurrent intensities $I(Ge_{3d})$, $I(Ge_{2p})$, and $I(Si_{2p})$, due to electrons emitted respectively from Ge($3d$), Ge($2p$), and Si($2p$) core levels, were collected by means of a concentric hemispherical analyzer in the direction perpendicular to the (001) surface. We have verified that in our experimental conditions, photoelectron diffraction effects are negligible.

III. EXPERIMENTAL RESULTS

In Figs. 1(a)–1(c) and Figs. 1(d)–1(f), we display the AFM images of three representative samples belonging to series A and B, respectively. The samples are [(a) and (d)] uncapped or capped by a (b) 1.5-nm-thick and (e) 1.8-nm-thick or [(c)–(f)] 4.5-nm-thick silicon layer.

The quantitative analysis of the AFM images of all samples of series A (open symbols) and B (closed symbols) is reported in Fig. 2 as a function of the deposited capping layer thickness. In Fig. 2(a), we report the island density; in Fig. 2(b), the dome average volume: the volume of the shrinking pyramid, less than 5% of the total island volume, is thus excluded from the following analysis; in Fig. 2(c), the fraction of the sample surface area covered by islands $\rho_C(\theta_{Si})$ [thus, the island-free surface U covers an area fraction $\rho_U(\theta_{Si})=1-\rho_C(\theta_{Si})$]; and in Fig. 2(d), the average aspect ratio, defined as the ratio $\alpha=h/b$ between an individual island height h and its basewidth b. Typical values for the dome height and basewidth are $h\sim25$ nm and $b\sim100$ nm in uncapped samples, and $h\sim10$ nm and $b\sim220$ nm for $\theta_{Si}=4.5$.

In the uncapped samples of both series, most of the islands (about 80%) are dome shaped, with the island density

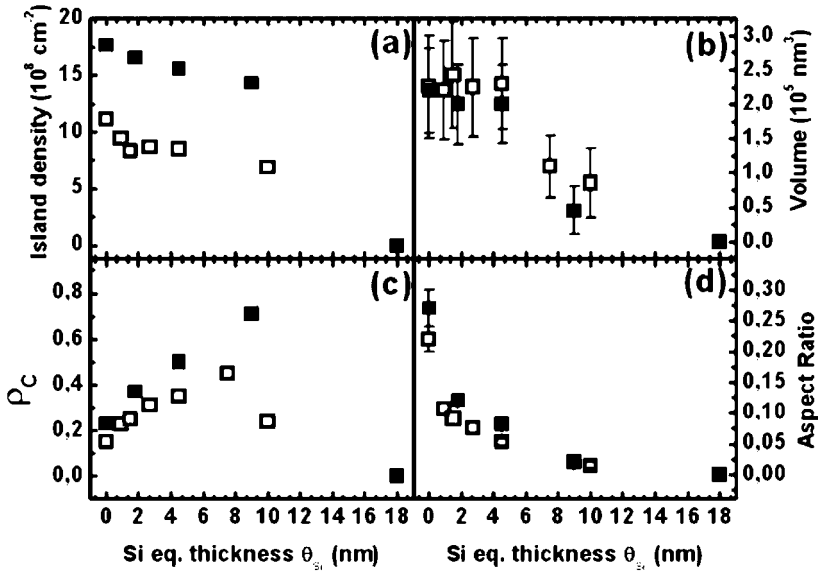

FIG. 2. Morphological data of series A (open symbols) and B (closed) as a function of the deposited silicon thickness. (a) Island density. (b) Average dome volume as measured by means of AFM. (c) Ratio of the projected surface occupied by the islands (two-dimensional island coverage). (d) Average aspect ratios of the islands. The standard deviation of the volume and aspect ratio distribution have been plotted as error bars. The uncertainty in the determination of the average dome volume of each sample is $\leqslant10\%$.

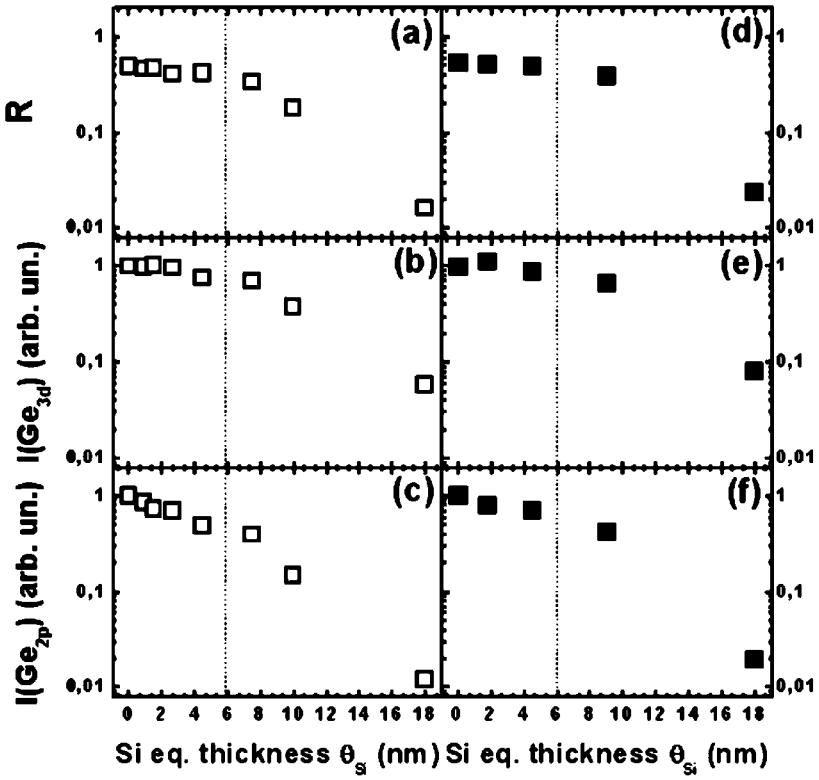

FIG. 3. XPS data of series A (open symbols, left) and B (closed, right) as a function of the amount of deposited silicon: [(a) and (d)] ratio of the photocurrent intensities $R=I(\mathrm{Ge}_{3d})/I(\mathrm{Si}_{2p})$; intensity of the photocurrent emitted from the [(b) and (e)] Ge_{3d} and [(c) and (f)] $I(\mathrm{Ge}_{2p})$ core levels. The data are normalized to the photocurrent intensity measured on the uncapped samples for each series.

of series B ~1.6 times higher. The average dome volume of the two samples coincides within 2%.

At the first stage of the Si capping, well-defined faceted structures are observed. In both series, the transformation of the island shape from higher domes to larger and flatter square-based pyramids with edges oriented along the [100]-equivalent directions is clearly seen. The deposition of a silicon layer as thin as $\theta_{\mathrm{Si}}=1$ nm is enough to induce the morphological transition, as witnessed by the island aspect ratio dropping to a value $\alpha=0.1$, typical of {105}-bound pyramids. An increased thickness of the capping layer promotes the formation of shallower three-dimensional structures covering a larger part of the surface.

The island density decreases by about 20% in both series because of the disappearance of the small pyramids. This implies that all the domes present on the uncapped samples "survive" the capping process, although they undergo the morphological evolution visible in Fig. 1. An interesting common feature of both series is that the AFM-measured average volume of the islands evolving from domes remains constant within the experimental error for Si capping layer thickness θ_{Si} below 5 nm. For larger quantity of deposited silicon, the island volume decreases sharply. This decrease is accompanied by the decrease of the surface area occupied by the islands and, eventually, of the island density. This evolution ends with the disappearance of the three-dimensional structures and the recovery of a flat morphology for $\theta_{\mathrm{Si}}=18$ nm. As we already reported, these observations give evidence of the development of a nonconformal silicon capping layer over the Ge(Si) islands[6,7] and are confirmed by the XPS measurements presented in Fig. 3 for both experimental series as a function of the deposited Si (left panels, series A; right panels, B). In the top panels, we report the ratio $R=I(\mathrm{Ge}_{3d})/I(\mathrm{Si}_{2p})$, while in the middle and bottom panels, we display the photocurrent intensities $I(\mathrm{Ge}_{3d})$ and $I(\mathrm{Ge}_{2p})$, respectively. Here, we point out that, owing to the large difference of the escape depth λ of Ge_{3d} and Ge_{2p} photoelectrons [$\lambda_{3d}=2.4$ nm (Ref. 18) and $\lambda_{2p}=0.5$ nm (Ref. 19) in our experimental conditions], the photocurrent intensities $I(\mathrm{Ge}_{3d})$ and $I(\mathrm{Ge}_{2p})$ are dependent on the Ge atomic distribution within the first 0–5 nm and 0–1 nm below the free surface, respectively. The behavior of R, $I(\mathrm{Ge}_{3d})$, and $I(\mathrm{Ge}_{2p})$ for increasing Si capping layer thickness observed in the two series is qualitatively similar. A strong decrease of all the three quantities is observed for Si cap-layer thickness θ_{Si} above 5 nm. This points to the formation of a Si layer of increasing thickness covering the sample regions where the Ge atoms are located.[6] Because of the smaller escape depth of photoelectrons emitted from Ge_{2p} core levels, the slope of the exponential decrease of the $I(\mathrm{Ge}_{2p})$ signal is higher than that of the $I(\mathrm{Ge}_{3d})$. Therefore, the AFM morphology is drastically influenced by the development of a "true" Si capping layer growing preferentially on the WL region. On the contrary, for $\theta_{\mathrm{Si}}<5$ nm, the R and the $I(\mathrm{Ge}_{3d})$ are almost constant. A decrease on the order of 30% is observed instead for the $I(\mathrm{Ge}_{2p})$ peak intensity. This behavior is compatible with the diffusion of most of the silicon atoms impinging on the surface inside the island layer and a redistribution of Ge atoms to larger area islands.[6]

In order to extract quantitative information on the intermixing process occurring during the island growth and at the first stage of the Si capping, we have calculated the expected $I(\mathrm{Ge}_{2p})$, $I(\mathrm{Ge}_{3d})$, and $I(\mathrm{Si}_{2p})$ and the ratio $R_{\mathrm{theo}}=I(\mathrm{Ge}_{3d})/I(\mathrm{Si}_{2p})$ starting from the actual sample morphologies as measured by AFM. The intensity of the electron flux photoemitted perpendicularly to the sample surface from a

given core level γ of Ge and Si atoms included in an infinitesimal volume $dV=dz_1dz_2dz_3$ is

$$dI(z_1,z_2,z_3) = I_0 N_{\mathrm{Ge,Si}}(z_1,z_2,z_3)\sigma_\gamma \times \exp\left(-\frac{t_{\mathrm{WL}} + d(z_1,z_2) - z_3}{\lambda_\gamma}\right) dz_1 dz_2 dz_3.$$

In this expression, z_1 and z_2 are the in-plane coordinates, while z_3 is the coordinate along the growth direction whose zero is located at the substrate-WL interface. I_0 accounts for the x-ray intensity and the analyzer collection efficiency, t_{WL} is the WL thickness, $d(z_1,z_2)$ is the height profile of the island layer emerging from the WL surface (i.e., the surface morphology as measured by AFM), σ_γ is the atomic cross section, λ_γ is the photoelectron escape depth, and $N_{\mathrm{Ge,Si}}(z_1,z_2,z_3)$ are the densities of Ge and Si atoms in dV. Since bulk Si and Ge have similar atomic densities N_0 in a random $Si_{1-x}Ge_x$ alloy we have $N_{\mathrm{Ge}}=N_{0X}(z_1,z_2,z_3)$ and $N_{\mathrm{Si}}=N_0[1-x(z_1,z_2,z_3)]$. The theoretical expression for $I(\mathrm{Ge}_{2p}), I(\mathrm{Ge}_{3d}), I(\mathrm{Si}_{2p})$, and the ratio $I(\mathrm{Ge}_{3d})/I(\mathrm{Si}_{2p})$ can then be derived by integrating the previous expression over the sample volume once a particular Ge distribution $x(z_1,z_2,z_3)$ is considered. The details of the calculation performed on the basis of the AFM measured surface morphology are reported in Ref. 18. By comparing the theoretical values with the experimental data of Fig. 3, we could get information on the Ge distribution in the island layer and on the atomic processes that control its alloying.

Prior to a thorough analysis of the diffusion and alloying processes occurring at the first stage of the Si deposition ($\theta_{\mathrm{Si}}<5$ nm), we discuss in the next section the morphology and the Ge distribution of the island layer in uncapped samples.

IV. SiGe INTERMIXING DURING ISLAND GROWTH

The most noticeable impact of the growth rate F on the development of the island layer is the difference between island density $n_A=1.2\times10^9$ cm^{-2} and $n_B=1.8\times10^9$ cm^{-2} for the samples of series A and B, respectively. This observation is compatible with the model of Sullivan *et al.*[20] predicting the density to increase as $n\propto F^{0.41}$ in experimental conditions similar to those used here (we found a best fit exponent of 0.46). The growth rate was not increased further to prevent island-island interaction from playing a major role on the island growth dynamics and on the intermixing process.[21] In order to investigate the intermixing occurring at the same stage of the island evolution, we tuned the deposition time in order to have similar island shape distribution in the two samples (relative frequency of domes and pyramids) as well as similar island volume.

We have seen that the expected XPS signals can be predicted based on calculations taking the island morphology as an input. In a previous work, we have evaluated from the XPS intensity ratio R the amount of SiGe intermixing during the island layer growth at different temperatures.[18] We assumed a homogeneous Ge distribution in the whole epilayer [$N_{\mathrm{Ge}}=N_{0x}$ and $N_{\mathrm{Si}}=N_0(1-x)$ in the islands and in the WL, $N_{\mathrm{Ge}}=0$ and $N_{\mathrm{Si}}=N_0$ in the substrate] and that the WL thickness scales with the layer composition as $t_{\mathrm{WL}}(\mathrm{Ge}_x\mathrm{Si}_{1-x}) \propto 1/x$.[22] Here, we improve this XPS-AFM model by assuming a nonhomogeneous Ge distribution with distinct average Ge contents in the islands (x) and in the WL (y).

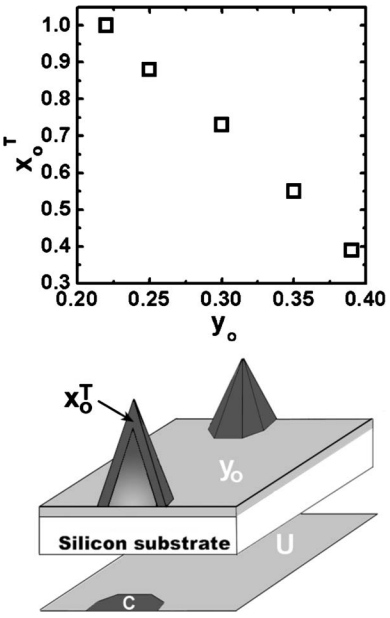

FIG. 4. x_0^{T} values of the Ge composition of the outer part of the islands as a function of the corresponding Ge composition of the wetting layer y_0. In the bottom part of the figure, we show a schematic of the sample morphology indicating the nomenclature as used in the main text: higher Ge content corresponds to darker regions.

The estimation of these parameters from the model will result particularly accurate for the uncapped sample of series A since, in this case, we have independently determined by means of transmission electron microscopy (TEM) and extended x-ray-absorption fine structure (EXAFS) measurements the WL thickness $t_{\mathrm{WL}}^{\mathrm{A}}\sim1.6$ nm and the average Ge content in the whole epilayer (islands+WL) $\langle\mathrm{Ge}\rangle_0^{\mathrm{A}}\sim0.5$.[23] The knowledge of $t_{\mathrm{WL}}^{\mathrm{A}}$ allows us to calculate, given the island morphology measured by AFM, the expected intensity ratio $R_{\mathrm{theo}}(x,y)=I(\mathrm{Ge}_{3d})/I(\mathrm{Si}_{2p})$ as a function of the Ge content in the islands (x) and in the WL (y) without further assumptions or fitting parameters. By equalizing the R_{theo} expression to the measured value $R^{\mathrm{A}}(0)=0.48$ [see Fig. 3(a)], the only coupled (x,y) pairs compatible with the experimental XPS data can be derived. Notice that, since the XPS signals originate from atoms within the first 5 nm below the sample surface, the y values are representative of the average concentration y_0 in the wetting layer ($t_{\mathrm{WL}}<\lambda$), while the x values are representative of the Ge content x_0^{T} in the outer crust of the islands (extending ~5 nm below the surface, see Fig. 4). The Ge concentration of this region is expected to be higher than the average composition x_0 of the whole island. As a matter of fact, Malachias *et al.* have nicely demonstrated, for Ge/Si islands deposited at 600–700 °C, that the Ge contents are not homogeneous, with a Ge-rich island outer surface and

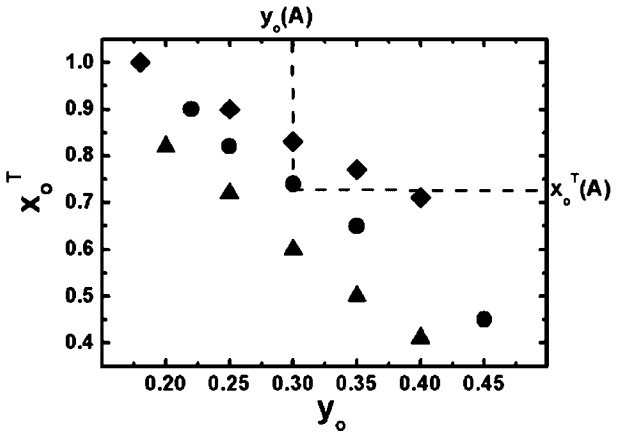

FIG. 5. Possible x_0^T values of the Ge composition of the outer part of the islands in the uncapped sample of series B as a function of the corresponding Ge composition of the wetting layer y_0. Data obtained with a WL thickness of the uncapped sample equal to $t_{WL}^B(0)=1.6$ nm (triangle), $t_{WL}^B(0)=1.2$ nm (circle), and $t_{WL}^B(0)=0.9$ nm (diamond). The values obtained in series A are reported here as limiting values (see text).

a Si-richer island core[24] of average composition $x_0^C<x_0$.

Infinite (x_0^T,y_0) coupled pairs inserted in the R_{theo} expression give the same $R_{theo}=R^A(0)$ value and are, therefore, compatible with our XPS result. However, since it is well established that at high growth temperature the WL is Si-richer than the islands (see Ref. 9 and references therein), we can assume in our model that $y_0<x_0^T<1$. Fixing $y_0=x_0^T=y_0^{Max}$ in the R_{theo} expression, $R_{theo}=R^A(0)$ gives $y_0^{Max}=0.38$, i.e., $y_0<0.38$. By imposing $x_0^T=1$ in the R_{theo} expression, we obtain the bottom limit $y_0^{Min}=0.23$. We find, therefore, $0.23<y_0<0.38$, that is, we can quantify the Ge content in the WL of the uncapped sample of series A to be $y_0=(0.30\pm0.05)$. On the contrary, the Ge content in the topmost part of the islands can be evaluated in a less accurate way as can be seen in Fig. 4, where the whole set of (x_0^T,y_0) values compatible with the experimental $R^A(0)$ value is reported. However, once the Ge content y_0 in the WL is established, the average Ge content in the islands x_0 can be derived from the EXAFS results in Ref. 23:

$$\langle \mathrm{Ge}\rangle_0^A=\frac{y_0V_{WL}^0+x_0V_{is}^0}{V_{WL}^0+V_{is}^0}=0.5,$$

where V_{WL}^0 and V_{is}^0 are the WL and the total island volume of the sample, respectively. The value $x_0\sim0.6$ obtained in this way represents a bottom limit for x_0^T and is, thus, consistent with $y_0\sim0.3$ obtained from XPS results ($x_0^T=0.73$ for $y_0=0.3$, see Fig. 4).

We have performed the same XPS-AFM analysis on the uncapped sample of series B deposited with a higher growth rate. Because TEM and EXAFS measurements were not available for this sample, in Fig. 5 we have reported the possible couples of (x_0^T,y_0) values compatible with the XPS $R^B(0)$ experimental result for different WL thickness: $t_{WL}^B(0)=1.6$ nm (triangle), $t_{WL}^B(0)=1.2$ nm (circle), and $t_{WL}^B(0)=0.9$ nm (diamond). The allowed (x_0^T,y_0) values and WL thickness can be further restricted on the basis of the values obtained for the uncapped sample of series A. As a matter of fact, a higher growth rate is expected to increase kinetic limitations and to reduce the intermixing, i.e., $y_0(B)\geq y_0(A)$ and $x_0^T(B)\geq x_0^T(A)$. Figure 5 shows that these constraints imply that the WL thickness in the uncapped sample of series B is $t_{WL}^B(0)\leq1.2$ nm $<t_{WL}^A(0)$. Tu and Tersoff[13] (TT) have recently developed a continuum model for mismatched heteroepitaxy that adequately accounts for intermixing between supplied atoms and substrate atoms in a surface layer of thickness w_s, where the atoms are sufficiently mobile to be in equilibrium with the surface. These authors found that both the critical composition and the critical thickness for the development of 3D islands are almost independent of the growth rate. On the contrary, we found that the WL thickness decreases for increasing growth rate. Bulk diffusion of atoms in the growth direction may be a possible explication for the disagreement of our results with the TT model. Indeed, the bulk diffusion is considered negligible in the TT model, while, in our experimental conditions, we can evaluate a bulk diffusion length ~1 nm,[25] i.e., greater than w_s [2–4 ML (monolayer), i.e., 0.3–0.6 nm]. It means that Si and Ge atoms mix in a layer of thickness $w_b>w_s$ below the surface. Contrary to w_s, w_b should depend on the growth rate F as $w_b\propto\sqrt{Dt_c}\propto\sqrt{D/F}$. In this expression, $t_c\propto1/F$ is the characteristic time scale for the growth at a rate F, and D is the bulk diffusivity. Because the WL thickness is expected to be proportional to w_b, we can, therefore, estimate $t_{WL}^B(0)=t_{WL}^A(0)\sqrt{F^A/F^B}\sim1.2$ nm.

Inspection of Fig. 5 indicates that for $t_{WL}^B(0)=1.2$ nm, $y_0(B)=0.3\sim y_0(A)$, i.e., in agreement with TT conclusions,[13] the WL composition does not depend on the growth rate. Moreover, the obtained WL composition $y_0=0.3$ is close to the estimation they made for the Ge/Si system. Our data, therefore, support the TT suggestion that the key factor controlling the crossover from planar growth to island formation is the continuous increase of the composition of the topmost part of the planar layer due to intermixing. Figure 5 also indicates that the Ge content in the topmost 5 nm of the islands is $x\sim0.74$, almost identical to the values obtained in series A. This suggests that the Ge content distribution in the islands is similar in the two samples, with an average island composition $x_0\sim0.6$, a composition of the island outer shell $x_0^T\sim0.75$, and an island core composition $0.3<x_0^C<0.6$. The independence of the island Ge distribution on the growth rate suggests that kinetic limitation is negligible in the intermixing process occurring during the island growth. This is not surprising at the deposition temperature $T_{dep}=750$ °C used here: as a matter of fact, Katsaros *et al.* have demonstrated that above 620 °C, the kinetic limitations to the strain-driven redistribution of the silicon atom incorporated during the formation of self-assembled islands are faded out.[16,26]

V. SiGe INTERMIXING DURING THE ISLAND CAPPING

We have seen that at the first stage of the sample capping ($\theta_{Si}<5$ nm), domes transform into pyramids in both sample series and that the AFM measured island volume does not

change in this shape transformation. We have to verify first that the volumes and shapes derived by AFM are representative of the actual intermixed islands. In fact, it was suggested that $V_{AFM}(\theta_{Si})$ can overestimate the island volume because of the development of a Si layer on top of the islands themselves.[16] As already stated, the $I(Ge_{2p})$ photocurrent is very sensitive to the deposition of a Si layer on top of the intermixed islands and, thus, can be used to probe whether the surface morphology displayed in Fig. 1 is that of bare intermixed islands, or the Si capping layer determines the shape and volume of the observed structures. Owing to the larger island coverage $\rho_C(B)$, XPS measurements on the samples belonging to series B are more sensitive to Si growth on top of the islands. Given the escape depth $\lambda_{2p} \sim 0.5$ nm, the development of a 1-nm-thick Si layer on top of the islands of this series during the capping process would reduce the $I(Ge_{2p})$ signal to much less than 50% of the signal measured on the uncapped sample.[27] On the contrary, we measure $I(Ge_{2p})_{\theta=4.5}/I(Ge_{2p})_{\theta=0}=0.7$ [see Fig. 3(f)]. It means that Si does not segregate on top of the islands and that the AFM images reported in Fig. 1 are representative of the true intermixed island morphology. This is in agreement also with the AFM results of Fig. 1 showing square-based islands oriented along the [100]-equivalent directions. In fact, it has been shown that when a silicon layer segregates on top of the islands, [110]-oriented square-based structures are observed.[7,16,17]

Once we have made clear that the AFM-measured morphology is that of intermixed islands, we can discuss its evolution under the capping process for $\theta_{Si} < 5$ nm. The main consequence of the previous discussion is that the island shape transformation induced by SiGe intermixing *truly* occurs at constant island volume as observed in Fig. 2. This characteristic is independent of the island density and coverage. Furthermore, because in both sample series the number of "large" islands is conserved and the volume of the disappearing small pyramids of the uncapped samples is negligible, both the large island volume and the total 3D volume of the island layer are conserved. The observed conservation of the total island volume provides insights into the atomic processes occurring during the Si capping of the island layer. As a matter of fact, when a given amount of silicon θ_{Si} is deposited over an uncapped island layer made of a WL of volume V^0_{WL} and total island volume V^0_{is}, the mass conservation implies that

$$V^0_{is} + V^0_{WL} + \theta_{Si} = V_{is}(\theta_{Si}) + V_{WL}(\theta_{Si}).$$

In this equation, $V_{is}(\theta_{Si})$ represents the total 3D volume measured by AFM, while $V_{WL}(\theta_{Si})$ is the volume of the intermixed WL extending from the Si substrate to the flat surface over which the islands lie. Since all the quantities studied here are proportional to the area of the analyzed surface, all volumes are expressed in equivalent thickness.

We measured by AFM, with a 10% accuracy, that in both series

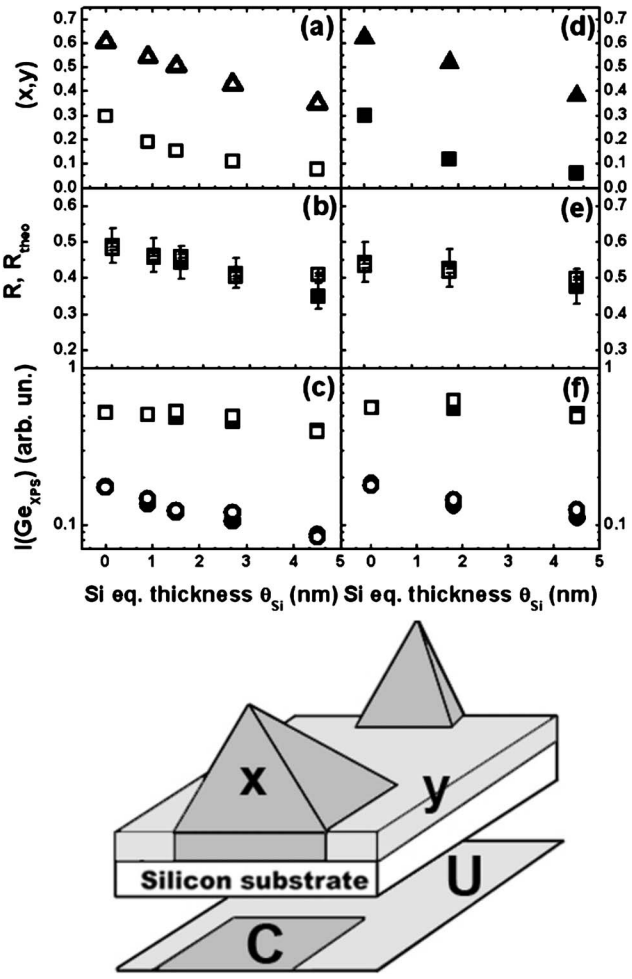

FIG. 6. Composition values and XPS data analysis reported for series A (left) and series B (right), as a function of the amount of deposited silicon: [(a) and (d)] Average Ge composition of the island (triangle) and the wetting layer (square), [(b) and (e)] values of the expected XPS ratio R_{theo} (closed symbol) and the measured XPS ratio R (open symbol), and [(c) and (f)] expected (closed symbols) and measured (open symbols) intensities of the $I(Ge_{2p})$ (circle) and $I(Ge_{3d})$ (square) photocurrents. In the bottom part of the figure, we show a schematic of the capped sample morphology annotated with the nomenclature we use in the main text.

$$V_{is}(\theta_{Si}) = V^0_{is}$$

and, therefore,

$$V_{WL}(\theta_{Si}) = V^0_{WL} + \theta_{Si}. \quad (1)$$

This simple derivation has important consequences: it implies that the thickness of the flat layer between islands increases by θ_{Si}, i.e., for any amount of silicon deposited on the U WL region (see sketches in Figs. 4 and 6), number of atoms equal to the number of Si atoms impinging on the island-free surface is incorporated. The more straightforward way to interpret this result is to assume that any surface migration between the islands and the U WL region is absent, be it for Ge or for Si atoms. The other scenario seems unlikely to occur. It implies that if a given number of Ge(Si) atoms moves from region C(U) to its complementary region,

at the same time *exactly the same number* of Si(Ge) atoms moves in the opposite direction even if the extensions of U and C regions are largely different and with different ratios in the two sample series.

We have verified the first hypothesis with our AFM-XPS model. Notice that in this framework the island volume, i.e., the volume of the 3D structures emerging from the WL surface, can be constant for increasing capping layer thickness because, despite the inclusion of Si atoms in the islands, there is a contemporary increase of the thickness of the WL which partially submerges the uncapped island bottom part. If we assume that the diffusion from islands to WL, and vice versa, is hindered and that Si is incorporated in the island layer, the average Ge content y in the "island-free" WL and the average Ge content x in the epilayer volume portion beyond the island surface can be calculated for any given θ_{Si} (see the sketch in Fig. 6). As a matter of fact, the average Ge content $\langle Ge\rangle$ in the whole epilayer (C+U regions) depends on the average Ge content $\langle Ge\rangle_0=(y_0V^0_{WL}+x_0V^0_{is})/(V^0_{WL}+V^0_{is})$ of the uncapped sample, θ_{Si}, x, y, and the island coverage $\rho_C(\theta_{Si})$ as follows:

$$\langle Ge\rangle = \frac{\langle Ge\rangle_0}{1+\dfrac{\theta_{Si}}{V^0_{WL}+V^0_{is}}} = \frac{yV_{WL}(\theta_{Si})[1-\rho_C(\theta_{Si})]+x[\rho_C(\theta_{Si})V_{WL}(\theta_{Si})+V_{is}(\theta_{Si})]}{V_{WL}(\theta_{Si})+V_{is}(\theta_{Si})},$$

where we have used the normalization condition $\rho_U(\theta_{Si})=1-\rho_C(\theta_{Si})$.

Given the Ge content y_0 in the WL of the uncapped sample, one can easily derive the (x,y) values for a given Si coverage as

$$y(\theta_{Si}) = \frac{y_0}{1+\theta_{Si}/V^0_{WL}}, \tag{2}$$

$$x(\theta_{Si}) = \frac{\dfrac{\langle Ge\rangle_0}{1+\dfrac{\theta_{Si}}{V^0_{WL}+V^0_{is}}}[V_{WL}(\theta_{Si})+V_{is}(\theta_{Si})]-yV_{WL}(\theta_{Si})[1-\rho_C(\theta_{Si})]}{[\rho_C(\theta_{Si})V_{WL}(\theta_{Si})+V_{is}(\theta_{Si})]}. \tag{3}$$

We used the (x,y) values obtained from Eqs. (1)–(3) calculate, for any θ_{Si}, the expected XPS signal intensities given the AFM morphology. Since the $\langle Ge\rangle_0^{A,B}$ and $y_0^{A,B}$ values have been determined in Sec. IV, these calculations do not contain fitting parameters. The use of the (x,y) average values [Eqs. (2) and (3)] to calculate the XPS intensities is justified because the Ge distribution in the islands is expected to become more homogeneous once the island layer has been exposed to a silicon flux. Indeed, during the capping, silicon atoms interdiffuse from the island-free surface and compensate the Ge composition gradient developed during the island growth (compare the sketches in Figs. 4 and 6). Furthermore, the increased intermixing and the induced island shape transformation reduce the strain inhomogeneity inside the islands, which, in turn, could induce an inhomogeneous Ge distribution. The expected XPS intensities are compared with the experimental values for each silicon coverage in Fig. 6 for both series A (left panel) and series B (right panel). In the top panel, we have reported the obtained x (triangle) and y (square) values evidencing the continuous dilution of the Ge content both in the islands and in the WL. The theoretical R_{theo} (closed square) and experimental R (open square) XPS intensity ratios have been reported in the middle panels as well as the expected (closed symbols) and measured (open symbols) $I(Ge_{2p})$ (circle) and $I(Ge_{3d})$ (square) intensities in the bottom panels.

The excellent agreement for both sample series, in the whole analyzed range, and for all the XPS quantities supports the hypothesis that for $\theta_{Si}<5$ the diffusion of atoms from the U (C) toward the C (U) regions is hindered and that the Ge distribution, both within the islands and the wetting layer, is homogeneous. Furthermore, it confirms the correctness of the uncapped sample x_0, y_0, and t_{WL} values determined in the previous section for series A and B.

The observed island layer evolution upon capping can be understood having in mind the following mechanism for the intermixing dynamics. Si atoms impinging on the U region deeply diffuse into the WL through missing dimer rows and lines.[26] The surface is (001) oriented and, thus, very little elastic relaxation is possible: the incorporation proceeds by means of local alloying with the help of the tendency of Ge atoms to "float" on the WL surface.[26] Our evidence is that this alloying process proceeds almost homogeneously over the thickness of several nanometers. Given the thickness of the WL, as determined in the previous section of this paper and using Eq. (1), we can estimate a WL thickness $t^A_{WL}(\theta_{Si}=4.5)=t^A_{WL}(\theta_{Si}=0)+4.5=6.1$ nm. A close inspection of cross sectional TEM of a completely capped sample, grown in conditions identical to those employed in series A, gives

$t_{WL} \sim 6-7$ nm,[28] in good agreement with the results presented here. The two data points can be compared since it was shown that the intermixing process is hindered after the formation of a continuous layer of silicon on top of the epilayer for capping temperatures up to 750 °C.[6,7] Therefore, the WL thickness and composition are expected to remain almost constant throughout further silicon deposition.[6] As far as the islands are concerned, Si atoms impinging on the island surface are strain driven toward the island edge. Ge atoms, mainly segregated into the topmost part of the islands, diffuse on the island surface to alloy with the incoming silicon atoms. This motion entails the observed island enlargement and the decrease of the island aspect ratio. We remind here that the island height immediately before the formation of the silicon overlayer is about 10 nm, i.e., about 1/3 of its "as-grown" height. Therefore, a large part of the island "core" is exposed to the external flux and, thus, involved in the intermixing process. An important consequence of this atomic redistribution is the increase of compositional homogeneity of the intermixing islands, as confirmed by the simultaneous agreement of the $I(Ge_{2p})$ and $I(Ge_{3d})$ signals with the results of our model [see Figs. 6(c) and 6(f)].

When the islands undergo the intermixing process, the effective mismatch is reduced. This stabilizes a lower aspect ratio and a larger basewidth. In fact, in this way the ratio of the island-free surface to projected area is reduced, with a consequent decrease of the surface energy and, thus, of the free energy.[3] The reverse Stranski-Krastanov shape evolution observed in Fig. 1 is in agreement with the shape stability diagram obtained assuming that the transition volume from domes to pyramids and from pyramids to prepyramids scales with the Ge content x in the islands as x^{-6}.[5,6] As a matter of fact, a stable pyramidal shape is predicted for the average island volume $V=2.2\times10^5$ nm^3 measured in our samples in the composition range $0.28<x<0.5$.

The absence of atom exchange between islands and WL proposed on the basis of our experimental data implies that the Ge content of WL in the U region becomes *lower* than the critical composition for 3D instability as predicted by the TT model. Some authors[15] suggest that this should promote the diffusion of Ge atoms belonging to the islands toward the WL region and that this motion is at the origin of the island size reduction they observe during the capping process. In contrast to the results of Refs. 15 and 16, we found that the domes present in the uncapped samples do not shrink during the capping, their volume being constant. We observed that only the small pyramids present in the uncapped samples disappeared upon capping (see Fig. 1), as shown by the slight decrease of the island density (about 20%), suggesting that the silicon capping entails the shrinking only of those islands having a volume smaller than a critical volume, as expected in an anomalous coarsening process.[29] On the other hand, we believe that the TT model, developed to describe the 2D-3D instability during island growth, is not adequate to follow the evolution of the island layer morphology and composition during capping. The capping process is completely different from the growth process. During Ge deposition, 3D islands nucleate once the strain accumulated in the WL is too large; the subsequently supplied Ge adatoms diffuse on the surface and are incorporated into the islands, increasing their volume. On the contrary, during the capping, the islands have already formed and have a large volume. While during the island growth the added material increases the Ge concentration and the stress, and, thus, the atom diffusivity, during the capping all these three quantities *decrease*. Furthermore, in the latter process, only Ge atoms belonging to a thin surface crust, thus having the possibility to diffuse on the surface, can be exploited to drive the shape evolution and to minimize the island energy. Both the surface diffusivity and the availability of Ge atoms decrease as silicon is incorporated into the island layer, slowing down the island enlargement and the alloying process.

Our data indicate that for $\theta_{Si}>5$ nm, the surface becomes Si-terminated and the residual strain modulation drives the dynamics of the subsequent silicon deposition. As a matter of fact, the silicon atoms can diffuse over the U and C regions and, given the residual tensile strain they experience over the islands, they preferentially bond in the U region, filling the space existing between the islands and, eventually, recovering a flat surface.[6] This is clearly shown by Figs. 2 and 3 as discussed in Sec. III of this paper. It is established that once the islands are completely covered, the bulk diffusion is not sufficient to drive a significant variation of the buried island composition.[6,7] Therefore, we expect that the composition of the buried island layers ($\theta_{Si}>5$ nm) is similar to that of the $\theta_{Si}=4.5$ nm sample, i.e., $x\sim0.35$ and $y\leqslant0.1$ [see Figs. 6(a) and 6(d)]. Taking into account the island layer morphology, these values are in agreement with the average composition of the buried island layer as determined by means of x-ray absorption spectroscopy on similar samples.[6]

VI. CONCLUSION

In this paper, we have presented the evolution of the composition and shape of self-assembled Ge/Si(001) islands during their growth and the subsequent Si capping at 750 °C.

We found that the WL composition of uncapped samples is $y_0\sim0.3$, substantially smaller than the island composition $x_0\sim0.6$, and that it is independent of the growth rate. This characteristic supports the idea[13] that the intermixing process is at the base of the 2D-3D transition. The observed decrease of the WL thickness upon doubling the growth rate suggests that at 750 °C, atomic bulk diffusion occurring close to the surface but along the growth direction plays a role in the intermixing process occurring during the development of the WL.

In capped samples, we found that the strain-driven Si-Ge intermixing occurs strongly at the early stage of the silicon deposition ($\theta_{Si}<5$ nm). This Si enrichment is accompanied by a reverse Stranski-Krastanov shape evolution. Our XPS-AFM data show unambiguously that island volume remains *constant* upon capping. This feature suggests the absence of atomic migration on the surface between the island region to the flat WL. The Ge content in the WL and in the islands, evaluated from the island morphology based on this assumption, reproduces very well the evolution under capping of the $R=I(Ge_{3d})/I(Si_{2p})$, $I(Ge_{2p})$, and $I(Ge_{3d})$ XPS data and

indicates that the observed reverse Stranski-Krastanov shape evolution follows the shape stability diagram obtained by assuming that the transition volume from domes to pyramids and from pyramids to prepyramids scale as x^{-6}. The intermixing proceeds until the islands and the wetting layer reach a composition of $x \sim 0.35$ and $y \sim 0.1$, respectively, and then fades out. For a deposited silicon thickness $\theta_{Si} > 5$ nm, the islands and the wetting layer are covered by a continuous silicon layer that, eventually, allows the system to recover a flat surface.

ACKNOWLEDGMENTS

Fruitful discussions with J. Tersoff, J. Witzens, L. Miglio, and F. Montalenti are gratefully acknowledged as well as the help of D. Spirito.

*Corresponding author; capellini@fis.uniroma3.it

[1] K. Brunner, Rep. Prog. Phys. **65**, 27 (2002).
[2] P. M. Petroff, A. Lorke, and A. Imamoglu, Phys. Today **54** (5), 46 (2001).
[3] M. De Seta, G. Capellini, F. Evangelisti, and C. Spinella, J. Appl. Phys. **92**, 614 (2002).
[4] C. Lang, D. J. H. Cockayne, and D. Nguyen-Manh, Phys. Rev. B **72**, 155328 (2005).
[5] A. Rastelli, M. Kummer, and H. von Känel, Phys. Rev. Lett. **87**, 256101 (2001).
[6] G. Capellini, M. De Seta, L. Di Gaspare, F. Evangelisti, and F. d'Acapito, J. Appl. Phys. **98**, 124901 (2005).
[7] M. De Seta, G. Capellini, L. Di Gaspare, F. Evangelisti, and F. d'Acapito, J. Appl. Phys. **100**, 093516 (2006).
[8] J. Stangl, A. Hesse, V. Holý, Z. Zhong, G. Bauer, U. Denker, and O. G. Schmidt, Appl. Phys. Lett. **82**, 2251 (2003).
[9] F. Ratto, G. Costantini, A. Rastelli, O. G. Schmidt, K. Kern, and F. Rosei, J. Exp. Nanosci. **1**, 279 (2006).
[10] M. Stoffel, A. Rastelli, S. Kiravittaya, and O. G. Schmidt, Phys. Rev. B **72**, 205411 (2005).
[11] G. Capellini, M. De Seta, F. Evangelisti, V. A. Zinovyev, G. Vastola, F. Montalenti, and Leo Miglio, Phys. Rev. Lett. **96**, 106102 (2006).
[12] M. Stoffel, A. Rastelli, J. Stangl, T. Merdzhanova, G. Bauer, and O. G. Schmidt, Phys. Rev. B **75**, 113307 (2007).
[13] Y. Tu and J. Tersoff, Phys. Rev. Lett. **93**, 216101 (2004).
[14] M. S. Leite, G. Medeiros-Ribeiro, T. I. Kamins, and R. S. Williams, Phys. Rev. Lett. **98**, 165901 (2007).
[15] C. Lang, S. Kodambaka, F. M. Ross, and D. J. H. Cockayne, Phys. Rev. Lett. **97**, 226104 (2006).
[16] G. Katsaros, A. Rastelli, M. Stoffel, G. Costantini, O. G. Schmidt, K. Kern, J. Tersoff, E. Müller, and H. von Känel, Appl. Phys. Lett. **89**, 253105 (2006).
[17] O. Kermarrec, Y. Campidelli, and D. Bensahel, J. Appl. Phys. **96**, 6175 (2004).
[18] G. Capellini, M. De Seta, and F. Evangelisti, Appl. Phys. Lett. **78**, 303 (2001).
[19] G. G. Jernigan, P. E. Thompson, and C. L. Silvestre, Surf. Sci. **380**, 417 (1997).
[20] J. S. Sullivan, E. Mateeva, H. Evans, D. E. Savage, and M. G. Lagally, J. Vac. Sci. Technol. A **17**, 2345 (1999).
[21] G. Capellini, M. De Seta, and F. Evangelisti, J. Appl. Phys. **93**, 291 (2003).
[22] S. N. Santalla, C. Kanyinda-Malu, and R. M. de la Cruz, Nanotechnology **15**, S215 (2004).
[23] From EXAFS measurements on series A uncapped sample exposed to air, we obtained an average germanium content $\langle Ge \rangle_{EXAFS} = 0.55$. This value corresponds to the average Ge content in the portion of the sample not oxidized. Because the thickness of the oxide layer is ~1 nm, the oxide portion of the sample corresponds to a large fraction of the WL and a small fraction of the island volume. As a consequence, if the Ge content in the WL is sensitively smaller than the Ge content in the islands as our result suggests, the value $\langle Ge \rangle_{EXAFS} = 0.55$ is something larger than the true average Ge content. Taking into account the presence of the oxide layer and assuming a Ge content in the WL $y_0 = 0.3$, we found $\langle Ge \rangle_0 \sim 0.5$.
[24] A. Malachias, S. Kycia, G. Medeiros-Ribeiro, R. Magalhaes-Paniago, T. I. Kamins, and R. S. Williams, Phys. Rev. Lett. **91**, 176101 (2003); G. Medeiros-Ribeiro, A. Malachias, S. Kycia, R. Magalhaes-Paniago, T. I. Kamins, and R. S. Williams, Appl. Phys. A: Mater. Sci. Process. **80**, 1211 (2005).
[25] Y. X. Dang, W. J. Fan, F. Lu, H. Wang, D. H. Zhang, and S. F. Yoon, J. Appl. Phys. **99**, 076108 (2006).
[26] D. B. Migas, P. Raiteri, Leo Miglio, A. Rastelli, and H. von Känel, Phys. Rev. B **69**, 235318 (2004).
[27] We have estimated the $I(Ge_{2p})$ signal ratio $I(Ge_{2p})_{\theta=4.5}/I(Ge_{2p})_{\theta=0}$ of series B if in the $\theta_{Si} = 4.5$ nm sample a 1-nm-thick silicon layer forms on top of the islands. Given the escape depth $\lambda_{2p} \sim 0.5$ nm, the development of a 1-nm-thick Si layer on top of the islands would reduce the island contribution to the signal intensity to ~1% of its original value. Therefore, in the $\theta_{Si} = 4.5$ nm sample, a fraction $\rho_C(\theta_{Si} = 4.5\ \text{nm}) = 0.5$ of the sample surface would not contribute to the $I(Ge_{2p})$ signal, in contrast to the uncapped sample where the entire surface contributes. Moreover, given $x_0^T > y_0$ and because of the GeSi intermixing in the U WL region upon capping, the average Ge content in the layer extending 1 nm below the entire surface (U+C) of the uncapped sample (the region from which the Ge_{2p} electrons can be collected) is expected to be higher than the average Ge content in the U region of the $\theta_{Si} = 4.5$ nm sample. Indeed, the Ge segregation, if any, occurs over just 2–3 ML $< \lambda_{2p} = 0.5$ nm (Ref. 26). As a consequence, a decrease of the $I(Ge_{2p})$ signal substantially larger than 50% of the signal measured on the uncapped sample is expected, i.e., $I(Ge_{2p})_{\theta=4.5}/I(Ge_{2p})_{\theta=0} \ll 0.5$.
[28] G. Capellini, M. De Seta, F. Evangelisti, and C. Spinella, Appl. Phys. Lett. **82**, 1772 (2003).
[29] A. Rastelli, M. Stoffel, J. Tersoff, G. S. Kar, and O. G. Schmidt, Phys. Rev. Lett. **95**, 026103 (2005).